



1 **VARIATION OF TOTAL ELECTRON CONTENT WITH SUNSPOT NUMBER**
2 **DURING THE ASCENDING AND MAXIMUM PHASES OF SOLAR CYCLE 24 AT**
3 **BIRNIN-KEBBI**

4 Aghogho Ogwala,^{1,*} Emmanuel Olufemi Somoye,¹ Olugbenga Ogunmodimu,³ Rasaanq
5 Adewemimo Adeniji-Adele,¹ Eugene Oghenakpobo Onori,¹ Oluwole Oyedokun ² and Ernest
6 Iheonu.¹

7 ^{1,*} Department of Physics, Lagos State University, Lagos, Nigeria.

8 ² Department of Physics, University of Lagos, Nigeria.

9 ³ Department of Electrical Engineering, Manchester Metropolitan University, United Kingdom.

10 **ABSTRACT**

11 Satellite radio signals are affected by the presence of electrons in the earth's upper atmosphere
12 (ionosphere). The more electrons in the path of the satellite radio signals, the more the impact on
13 the accuracy of satellite navigation systems such as the Global Positioning System (GPS)/ Global
14 Navigation Satellite System (GNSS) and GLONASS. These electrons introduce several meters
15 of error in position calculation. Total Electron Content (TEC) is used to monitor possible space
16 weather impacts on satellite to ground communication and satellite navigation. TEC is modified
17 in the ionosphere by changing solar Extreme Ultra-Violet (EUV) radiation, geomagnetic storms,
18 and the atmospheric waves that propagate up from the lower atmosphere. Therefore, TEC
19 depends on local time, latitude, longitude, season, geomagnetic conditions, solar cycle activity,
20 and condition of the troposphere. A dual frequency GPS receiver located at an equatorial station,
21 Birnin-Kebbi in Northern Nigeria (geographic location: 12.64°N; 4.22°E), has been used to
22 investigate variation of TEC during the period of 2011 to 2014. We investigate the diurnal,



23 seasonal and solar cycle dependence of GPS-TEC. The result shows that TEC increases from a
24 minimum at 0400 local time (LT) to maximum daytime peak between 1300 – 1600 LT and then
25 decreases to a minimum value after sunset for all the years. Slight post-noon peaks in the
26 daytime maximum and post-sunset decrease and enhancement is observed in some months. We
27 observed that TEC were higher in the equinoxes than the solstices only in 2012. Where as in
28 2011, September equinox and December solstice recorded higher magnitude followed by March
29 equinox and lowest in June solstice. In 2013, December solstice magnitude was highest,
30 followed by the equinoxes and lowest in June solstice. In 2014, March equinox and December
31 solstice magnitude were higher than September equinox and June solstice magnitude. June
32 solstice consistently recorded the lowest values for all the years.

33 **KEYWORDS:** TEC; variation; ascending phase; maximum phase; sunspot number; solar cycle
34 24.

35 **CORRESPONDING AUTHOR PHONE:** +234 8055650264

36 **CORRESPONDING AUTHOR E-MAIL:** ogwala02@gmail.com

37

38

39

40

41

42

43

44

45

46



47 INTRODUCTION

48 The ionosphere causes a variation in the intensity of radio signals – fading – as a result of
49 irregularities (inhomogeneity in electron density) (Somoye, 2010; Ogwala *et al.* 2018). Akala *et*
50 *al.*, (2011) reported that the variable nature of the equatorial/ low latitude ionosphere threatens
51 communication and navigation/ satellite systems. The equatorial/ low latitude ionosphere
52 exhibits many unique features such as the seasonal anomaly, semi-annual anomaly, equinoctial
53 anomaly, noon bite-out, spread-F, equatorial electrojet (EEJ), equatorial plasma bubbles (EPB),
54 etc.

55 For many decades, scientists have been studying these ionospheric features and the role
56 they play in trans-ionospheric electromagnetic radio wave propagation. These studies are being
57 carried out using different techniques and instruments. Some of the instruments are: (i)
58 ionosonde: which provides worldwide determination of ionospheric parameters with high
59 reliability, but these are limited to the bottom-side of the ionosphere (Ciraolo and Spalla, 2002),
60 (ii) incoherent scatter radar: a technique for detecting and studying remote targets (elections) by
61 transmitting radio waves in the direction of the target at high speed. They are also limited to the
62 bottom-side of the ionosphere (Zhang and Holt, 2008) and (iii) GPS receivers: provide direct
63 measurements from satellites. Their sounding capacity extends to the topside of the ionosphere,
64 but are affected by time and space constraints (Ciraolo and Spalla, 2002). Recently, GPS
65 receivers are the most efficient method used to eliminate the effect of the ionosphere on radio
66 signals. This method combines signals in different L band frequencies, L1 (1575 MHz) and L2
67 (1228 MHz).

68 Almost all space geodetic techniques transmit signals in at least two different frequencies
69 for better accuracy (Alizadeh *et al.*, 2013). These are combined linearly and can greatly eliminate



70 the effect of the ionosphere on radio signals. When Global Navigation Satellite System (GNSS)
71 signals propagate through the ionosphere, the carrier experiences phase advance and the code
72 experiences a group delay due to the electron density along the line of sight (LOS) from the
73 satellite to the receiver (Bagiya *et al.*, 2009; Tariku, 2015). Thus, the carrier phase pseudo ranges
74 are measured too short, and the code pseudo ranges are measured too long compared to the
75 geometric range between the satellite and the receiver. This results in a range error of the
76 positioning accuracy provided by a GPS receiver. The range error due to TEC in the ionosphere
77 varies from hundreds of meters at mid-day, during high solar activity when the satellite is near
78 the horizon of the observer, to a few meters at night during low solar activity, with the satellite
79 positioned at zenith angle (Bagiya *et al.*, 2009). It is documented that ionospheric delay which is
80 proportional to TEC is the highest contributor to GPS positioning error (Alizadeh *et al.*, 2013;
81 Akala *et al.*, 2013).

82 In the past few decades, studies on the temporal and spatial variations of TEC have
83 gained popularity in the scientific community (Wu *et al.*, 2008). However, understanding the
84 temporal and spatial variation of TEC will also go a long way in obtaining the positioning
85 accuracy of GNSS under disturbed and quiet conditions.

86 The global distribution of TEC variations and its characteristics at all latitudes, during
87 different solar cycle phases under disturbed and quiet conditions have been investigated by many
88 researchers (Bhuyan and Borah, 2007). It is reported that the differential carrier phase advance on
89 single frequency carrier phase observations can be at the decimeter level for baseline lengths of
90 40 km (Kleusberg, 1986). In 1995, the US Department of Defence (DOD) developed a GPS
91 receiver which operates two simultaneous frequency bands (L1 and L2) to augment the single
92 frequency receiver (Bolaji *et al.* 2012).



93 Due to the dispersive nature of the ionosphere, the time delay between the two
94 frequencies of a GNSS signal as it propagates through the ionosphere is given Equation (1) as
95 $\Delta t = t_2 - t_1$. Thus,

$$96 \quad \Delta t = \left(\frac{40.3}{c}\right) \times \frac{TEC}{\left[\left(\frac{1}{f_2^2}\right) - \left(\frac{1}{f_1^2}\right)\right]} \quad (1)$$

97 Where c is speed of light. Hence, Δt measured between the L1 and L2 frequencies is used to
98 evaluate TEC along the ray path. By measuring this delay using dual frequency GPS receivers,
99 properties of the ionosphere can be inferred and used to monitor space weather events such as
100 GNSS, HF communications, Space Based Observation Radar and Situational Awareness Radar,
101 etc.

102 TEC from satellite to receiver in the ionosphere is defined by Equation (2). It is measured
103 in multiples of TEC units ($1 \text{ TECU} = 10^{16} \text{ el/m}^2$)

$$104 \quad TEC = \int n_e(s) ds \quad (2)$$

105 Rama Rao *et al.* (2006a, b) reported maximum day-to-day variability in TEC at the EIA
106 crest regions, increasing peak value of TEC with increase in integrated equatorial electrojet
107 (IEEJ) strength, maximum monthly average diurnal variations during equinox months followed
108 by winter months and lowest during summer months. They also reported positive correlation of
109 TEC and EEJ and the spatial variation of TEC in the equatorial region. Titheridge (1974)
110 attributed the lower TEC values during the summer seasons to low ionization density resulting
111 from reduced O/ N₂ ratio (production rates) which is a result of increased scale height. Bhuyan
112 and Borah (2007) compared TEC derived from GPS receivers with IRI in the Indian sector and
113 inferred that the diurnal amplitude of TEC is higher during the equinoxes followed by December
114 solstices and lowest in June solstice, i.e., observing winter anomaly in seasonal variation. Akala



115 *et al.* (2013) on the comparison of equatorial GPS-TEC observations over an African station and
116 an American station during the minimum and ascending phases of solar cycle 24 reported that
117 seasonal VTEC values were maximum and minimum during March equinox and June solstice
118 respectively, during minimum solar cycle phase at both stations. They also reported that during
119 the ascending phase of solar cycle 24, minimum and maximum seasonal VTEC values were
120 recorded during December solstice and June solstice respectively.

121 In this research, the result obtained in 2012 and 2013 which corresponds to the result of
122 these researchers. However, the result we obtained in 2011 and 2014 did not follow the trend
123 reported by these researchers, who explored the equatorial/ low latitude during different solar
124 cycle epochs.

125

126 DATA AND METHODOLOGY

127 2.1 DATA

128 The Receiver Independence Exchange (RINEX) GPS data files were downloaded daily
129 from NIGNET website (www.nignet.net) and processed using Bernese software and GPS TEC
130 analysis software. The GPS TEC analysis software reads raw data, processes cycle slips in phase
131 data, reads satellite biases from the International GNSS services (IGS) code files (and calculates
132 them if unavailable), and calculates receiver bias, inter-channel biases for different satellites in
133 the constellation. Effect due to multipath is eliminated by using a minimum elevation angle of
134 20°.

135 GPS TEC obtained from the TEC analysis software is the STEC. STEC is polluted with
136 several biases that must be eliminated to get VTEC. VTEC is calculated from the daily values of
137 STEC using equation (3).



138 $VTEC = STEC - [b_R + b_S + b_{RX}]/S(E)$ (3)

139 Where b_R , b_S , and b_{RX} are receiver bias, satellite bias receiver interchannel bias respectively.
 140 $S(E)$, which is the oblique factor with zenith angle, z at IPP (Ionospheric Pierce Point) is
 141 expressed in equation (4).

142 $S(E) = \frac{1}{\cos(z)} = \left\{ 1 - \left(\frac{R_E \times \cos(E)}{R_E + h_S} \right)^2 \right\}^{-0.5}$ (4)

143 R_E = the mean radius of the earth in km and h_S = ionospheric height from the surface of the earth.

144 Hourly VTEC data obtained from these processing software are averaged to daily TEC
 145 values in TEC units ($1 \text{ TECU} = 10^{16} \text{ el/m}^2$). TEC from Birnin-kebbi, on geographic Latitude
 146 12.47°N and geographic Longitude 4.23°E located in Northern Nigeria, obtained during the
 147 period 2011 – 2014, which corresponds to the ascending (2011 – 2013) and maximum (2014)
 148 phases of solar cycle 24 were used. Solar cycle 24 is regarded as a quiet solar cycle which
 149 peaked in 2014 with maximum sunspot number (103) occurring in February. Values of sunspot
 150 number, R_z , in Text format were obtained from Space Physics Interactive Data Resource
 151 (SPIDR) website (www.ionosonde.spidr.com). Table 1 shows the years used in this study and
 152 their corresponding sunspot number, R_z .

153 Table I: Table of years, solar cycle phase and sunspot number, R_z [Source: Author].

Years	Solar Cycle Phase	Sunspot Number, R_z
2011	Ascending	55.7
2012	Ascending	57.6
2013	Ascending	64.7
2014	Maximum	79.6

154

155



156 2.2 METHODOLOGY

157 Diurnal variations were analysed using the monthly mean values of VTEC with respect to
158 local time (LT). The annual variation of TEC were plotted against all hours from the first day of
159 January to the last day of December for the years under investigation (2011 – 2014). The data
160 was grouped following Onwumechilli and Ogbuehi (1964) into four seasons namely: March
161 equinox (February, March and April), June solstice (May, June and July), September equinox
162 (August, September and October) and December solstice (November, December and January), in
163 order to investigate seasonal variation. Finally, Annual variation of TEC and sunspot number, Rz
164 were also analysed by plotting mean TEC and mean Rz against each month of the year.

165 RESULT AND DISCUSSIONS

166 Figures 1 to 4 shows the diurnal variation of GPS TEC in the Nigerian Equatorial
167 Ionosphere (NEI) for the years 2011 to 2014 respectively, were represented by data obtained
168 from the GPS receiver installed at Birnin-Kebbi station. The diurnal variation of GPS TEC
169 reveals the typical characteristics of an equatorial/ low latitude ionosphere. Generally, day-to-day
170 TEC variation is higher during the daytime than nighttime for all the years. The diurnal variation
171 shows TEC rising rapidly from a minimum just before sunrise between 03:00 – 05:00 LT (~2
172 TECU) in 2011, 04:00 – 05 LT (~3 TECU) in 2012, 03:00 – 05:00 LT in 2013 (~3 TECU), and
173 03:00 – 05:00 LT in 2014 (~3 TECU). TEC is found to increase to a broad daytime maximum
174 between 00:12 LT – 00:16 LT in all years before falling to a minimum after sunset. The steep
175 increase in TEC has been attributed to the solar EUV ionization together with the upward
176 vertical $E \times B$ resulting from the rapid filling up of the magnetic field tube at sunrise (Dabas *et*
177 *al.*, 2003; Somoye *et al.*, 2011; Hajra *et al.* 2016; D'ujanga *et al.*, 2017) and meridional winds
178 (Suranya *et al.*, 2015). These magnetic field tubes collapse after sunset due to low thermospheric



179 temperature and Releigh Taylor Instability (RTI) (Ayorinde *et al.*, 2016) giving rise to the
180 minimum TEC values after sunset. These results are similar to findings of Bolaji *et al.*, (2012),
181 Fayose *et al.*, (2012), Okoh *et al.*, (2014), Eyelade *et al.*, (2017) who have explored the NEI.

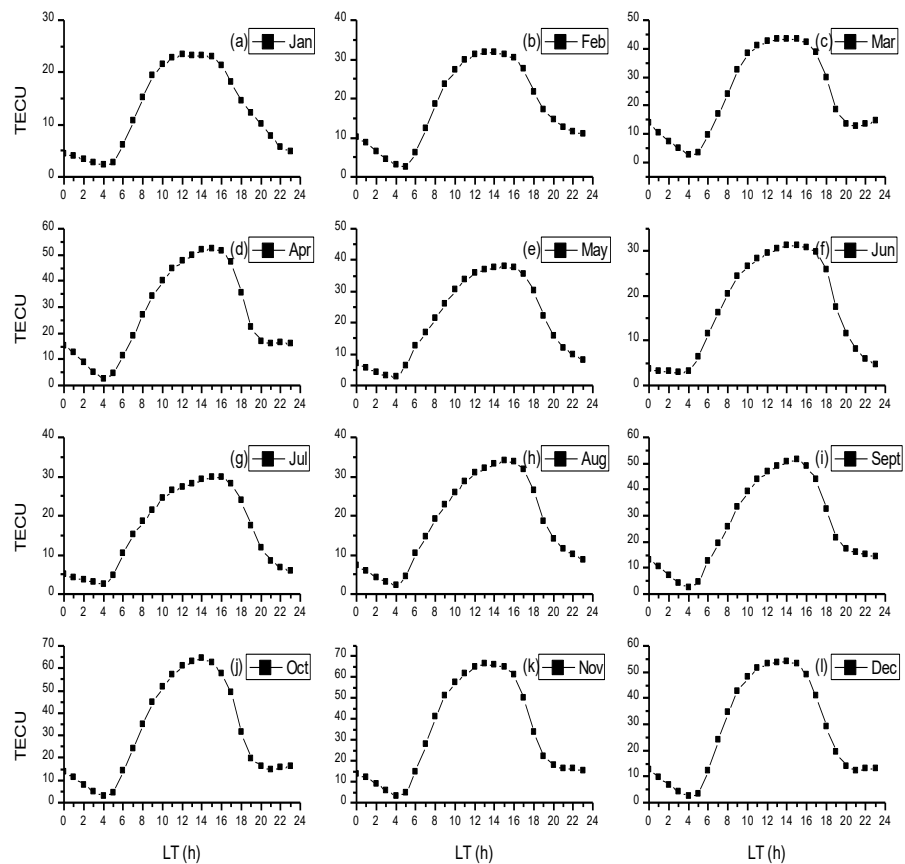


Figure 1: Diurnal variation of VTEC in each month during January – December 2011 at Birnin-Kebbi

182

183

184

185

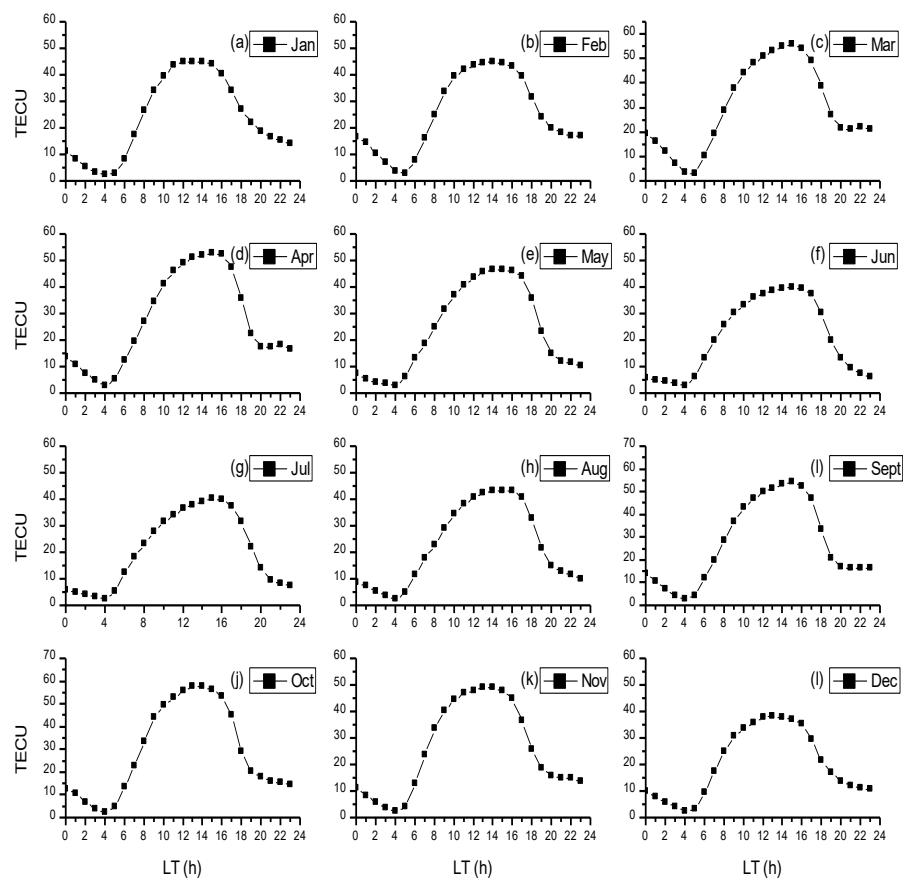


Figure 2: Diurnal variation of VTEC in each month during January – December 2012 at Birnin-Kebbi

186

187

188

189

190

191

192

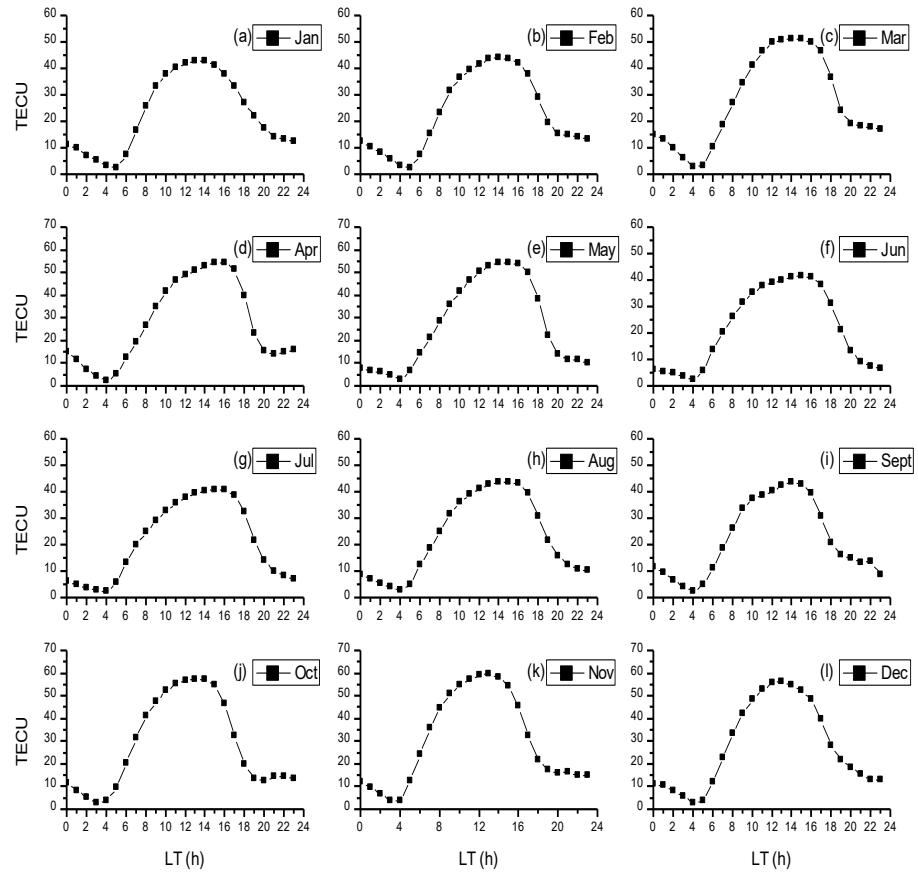


Figure 3: Diurnal variation of VTEC in each month during January – December 2013 at Birnin-Kebbi

193

194

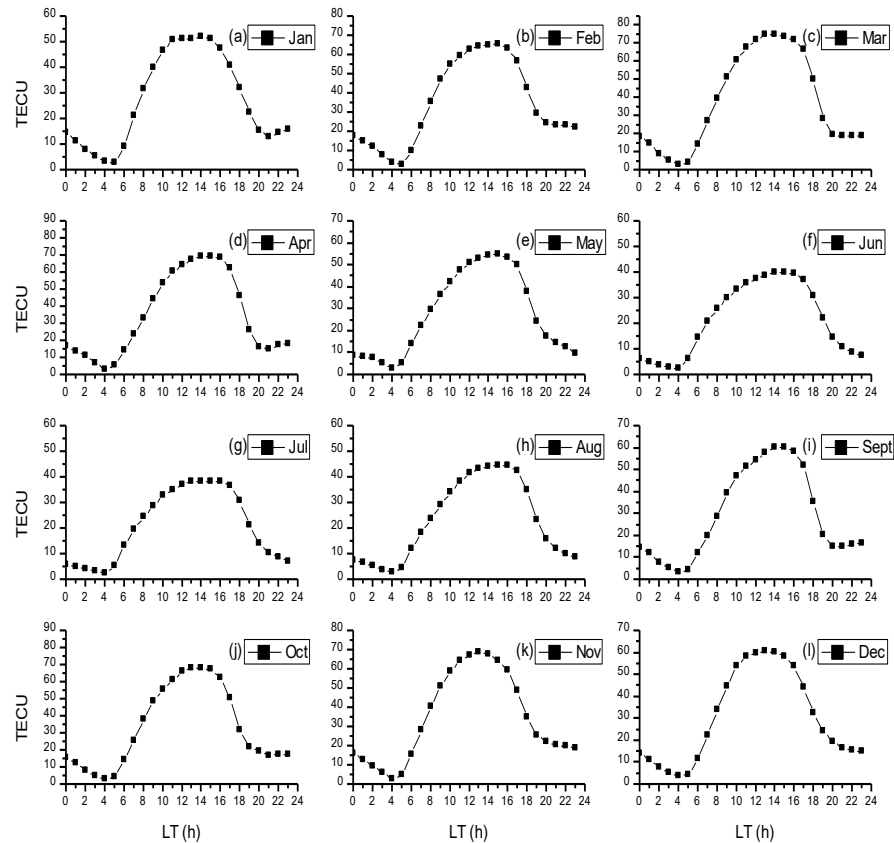
195

196

197

198

199



200 Figure 4: Diurnal variation of VTEC in each month during January – December 2014 at
 201 Birnin-Kebbi

202 It can be seen from the Figures that TEC was much higher in 2014 with maximum values
 203 up to 75 TECU in March. The diurnal variation reveals that the peak of TEC of some months
 204 were delayed till after noon. For example, the months of April, July, August and September in
 205 2011, March, April, June and September in 2012, April, June, July and September in 2013 had
 206 delayed peak. The delayed TEC peak were also seen in April, May, June, August and September
 207 of 2014. This type of peak shifting is peculiar to the Polar Regions and it is found to depend on

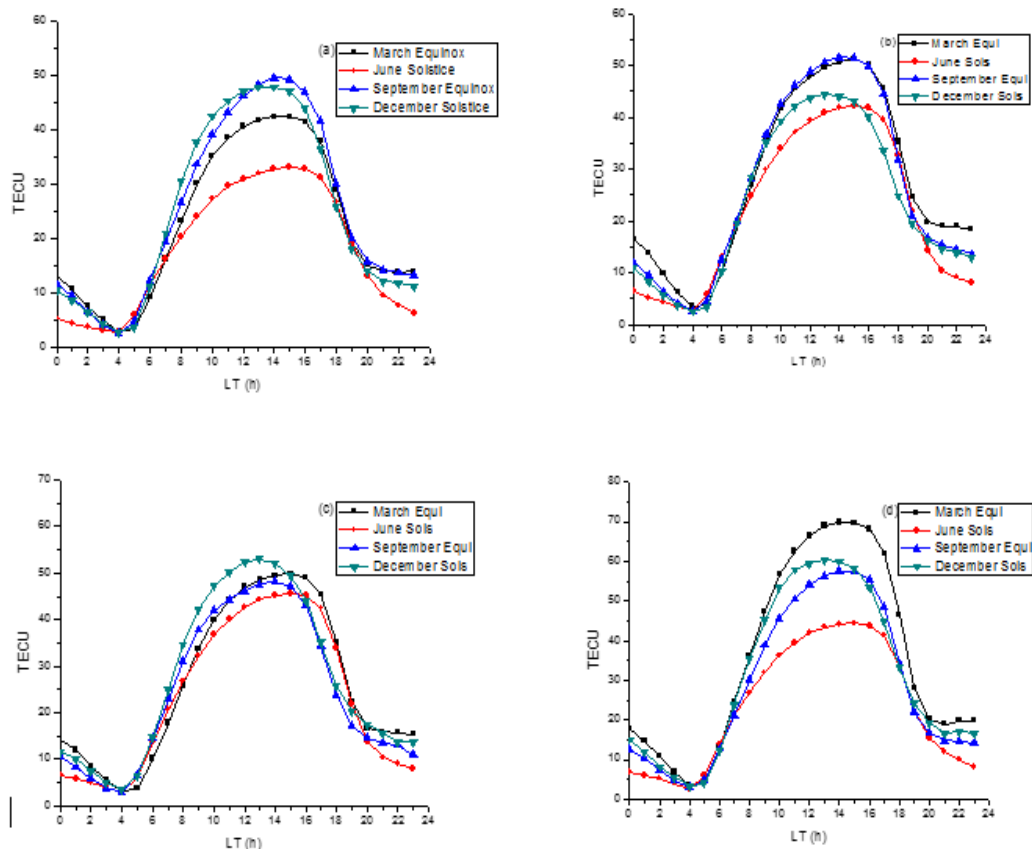


208 the solar zenith angle. Another major phenomenon seen in the diurnal variation of TEC is the
209 post-sunset decrease and slight enhancement in some months. The nighttime enhancement of
210 TEC, for example, March, April and October of the year 2011, March and April of the year
211 2012, March, April, September and October of the year 2013, January, April and September of
212 the year 2014 was documented by previous researchers like Rama Rao *et al.*, 2009; D'ujanga *et*
213 *al.*, 2017. They attributed it to the product of eastward and westward directed electric field which
214 produces an upward and downward motion of ionospheric plasma during the day and night
215 respectively.

216 Figure 5 plots the seasonal variations of TEC for the four years under investigation. The
217 change in concentration of Oxygen and molecular Nitrogen have been reported to be the main
218 cause of seasonal variation of ionospheric parameters. Seasonal variation of TEC in this study
219 depicts semi-annual variation with equinoctial maximum (~ 51 TECU) and solstitial minimum
220 (~ 44 TECU) in 2012. D'ujanga *et al.*, (2017) reported that since the sun passes through the
221 equator during the equinox, both March and September equinox experience the same solar
222 radiation. It is also a well established fact that March 20 and September 23 are the only times in
223 the year when the solar terminator is perpendicular to the equator, giving rise to the equinoctial
224 maximum. The semi-annual variation has been attributed to the effect of solar zenith angle and
225 magnetic field geometry (Wu *et al.*, 2004; Rama Rao *et al.*, 2006a). Another important feature of
226 ionospheric parameters (known as equinoctial asymmetry) as reported in the work of Bolaji *et*
227 *al.*, (2012); Akala *et al.*, (2013); Eyelade *et al.*, (2017); D'ujanga *et al.*, (2017); Aggarwal *et al.*,
228 (2017) and others, is clearly seen in all years used in this work. Akala *et al.*, (2013) also reported
229 minimum and maximum seasonal VTEC values during December solstice and June solstice
230 respectively, during ascending phase of solar cycle 24. Equinoctial asymmetry is a strong



231 phenomenon in low latitudes (Aggarwal *et al.*, 2017). The equinoctial asymmetry has been
232 explained in terms of the differences in the meridional winds leading to changes in the neutral
233 gas composition during the equinoxes.



234 Figure 5: Seasonal variation of TEC during (a) 2011 (b) 2012 (c) 2013 and (d) 2014
235

236 In 2011 and 2014, the seasonal variation of TEC in the ionosphere did not follow the
237 pattern reported by these researchers. In 2011, September equinox and December solstice
238 recorded higher magnitude, followed by March equinox, the lowest was in June solstice. In 2013,
239 December solstice magnitude was highest, followed by the equinoxes, March and September
240 respectively and lowest in June solstice. This corresponds to result obtained by Akala *et al.*



241 (2013), which they attributed to increase in ion production rate in winter season and anti-
242 correlation between December and June Solstice pre-reversal velocity enhancement. In 2014,
243 March equinox and December solstice magnitudes were higher than September equinox and June
244 solstice magnitudes. December solstice magnitude is found to occur between the magnitudes of
245 the equinoxes in 2011 and 2014. The September equinox magnitude and March equinox
246 magnitude are observed to interchange in 2011 and 2014. Overall, June solstice magnitudes were
247 lowest during all the years. This is due to low ionization resulting from reduced production rates,
248 i.e. O/ N₂ ratio (Titheridge 1974).

249 Figure 6 shows the plot of annual variation of TEC and sunspot number, R_z against the
250 months of the year for the four years. The plots reveal the strong dependence of TEC on solar
251 activity (sunspot number). TEC and sunspot number increased gradually from 2011 to 2014.
252 Although solar cycle 24 is regarded as a quiet solar cycle, which peaked in 2014, the sun erupted
253 with some few major flares in February and October of the same year (Kane, 2002). Hence,
254 February, October and November 2014 were months of highest TEC values. An X-class type
255 solar flare was reported in February of 2011, resulting in a high value of sunspot number.
256 Increase in the sun's activities increases the number of electrons along the line of sight (LOS)
257 from a satellite to receiver on ground.

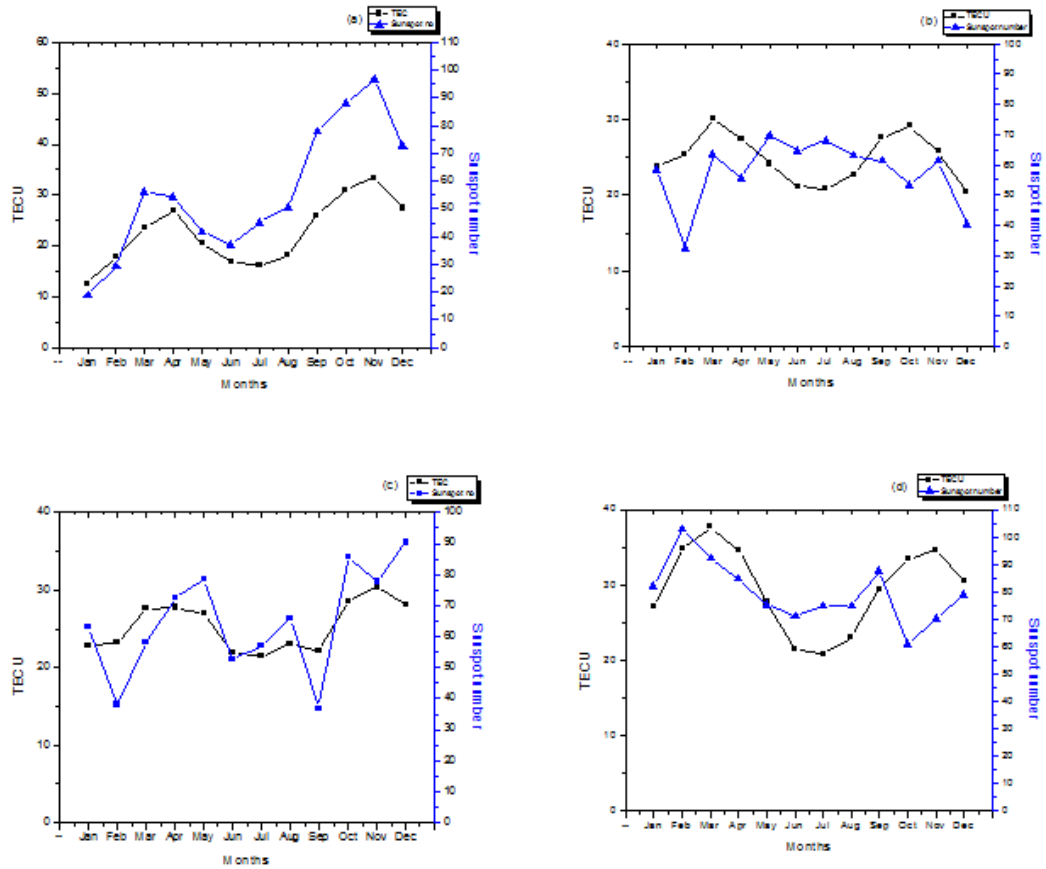
258

259

260

261

262



263

Figure 6: Annual variation of TEC and sunspot number, Rz during (a) 2011 (b) 2012 (c) 2013 and (d) 2014.

264

265 High solar activity produces solar flares of varying classes. As solar particles crash with
266 nitrogen and oxygen atoms in the upper atmosphere, these classes of flares produce waves of
267 ionization in the ionosphere that briefly alters the propagation of radio signals (Kane, 2002).
268 When solar flares become very intense, their electric field impulses, caused by disruption in the
269 earth's magnetic field due to ionization particles, may damage infrastructure such as power grids
270 and telephone lines not adequately protected against the geo-magnetically induced current (GIC),
271 leading to wastage of economic resources. Several earth-orbiting satellites may be in similar



272 danger. Hence, efforts are being made to develop tools and models from scientific results, to
273 forecast localised GIC impacts in national infrastructure. This forecasting capability will provide
274 operators with the information required to make swift operational decision, which may include
275 cancelling maintenance work or re-routing load in order to protect national infrastructure.
276 Operators will also advice when it is considered safe to resume normal operations.

277 CONCLUSIONS

278 Studies on TEC variations at Birnin-Kebbiin Northern Nigeria during the ascending and
279 maximum phases of solar cycle 24 have been carried out. The result obtained reveals the
280 following:

- 281 1. Higher TEC day-to-day variations during the daytime than nighttime for all the years
282 were observed. The diurnal variation shows TEC rising rapidly from a minimum just
283 before sunrise between 03:00 – 05:00 LT (~2 TECU) in 2011, 04:00 – 05 LT (~3 TECU)
284 in 2012, 03:00 – 05:00 LT in 2013 (~3 TECU), and 03:00 – 05:00 LT in 2014 (~3
285 TECU). TEC is found to increase to a broad daytime maximum between 00:12 LT –
286 00:16 LT for all years before falling to a minimum after sunset.
- 287 2. The diurnal variation reveals that the peak of TEC of some months were delayed till
288 after-noon. Post-sunset decrease and enhancement were also observed in the diurnal
289 variation of TEC in some months.
- 290 3. Seasonal variation of TEC in this study depicts semi-annual variation with equinoctial
291 maximum (~ 51 TECU), followed by December solstice magnitude (~ 44 TECU) and
292 least in June solstice seasons (~ 41 TECU) in 2012. This seasonal trend was not the case
293 for 2011, 2013 and 2014, though June solstice consistently recorded the lowest value for
294 all years.



295 4. Finally, annual variation of TEC and sunspot number, Rz against the months of the year
296 for the four years were plotted. The plots reveal the strong dependence of TEC on solar
297 activity (sunspot number). TEC and sunspot number were found to increase gradually
298 from 2011 to 2014.

299

300 **ACKNOWLEDGEMENT**

301 We thank the Office of the Surveyor General of the Federation (OSGoF) for making TEC data
302 available through the infrastructure www.nignet.net. We also thank Hatanaka, Y., Gopi Krishna
303 for providing TEC processing software online.

304

305 **REFERENCES**

306 Aggarwal, M., Bardhan, A., Sharma, D.K. (2017). Equinoctial asymmetry in ionosphere over
307 Indian region during 2006 – 2013 using COSMIC measurements. *Advances in Space Res.*, 60,
308 999 – 1014.

309 Akala, A.O., Somoye, E.O, Adeloje, A.B., Rabiou, A.B. (2011). Ionospheric f_oF_2 variability at
310 equatorial and low latitudes during high, moderate and low solar activity. *Indian Journal of*
311 *Radio and Space Physics*. Vol. 40, pp 124 – 129.

312 Akala, A.O., Seemala, G.K., Doherty, P.H., Valladares, C.E., Carrano, C.S., Espinoza, J., and
313 Oluyo, K.S. (2013). Comparison of equatorial GPS-TEC observations over an African station
314 and an American station during the minimum and ascending phases of solar cycle 24. *Ann.*
315 *Geophys.*, 31, 2085.



- 316 Alizadeh, M.M., Wijaya, D.D., Hobiger, T., Weber, R., Schuh, H. (2013). Ionospheric effects on
317 microwave signals in J. Bohm and H. Schuh (eds). Atmospheric Effect in Space Geodesy.
318 Springer atmospheric sciences. Doi: 10.1007/978-3-642-36932-2_2, © Springer-Verlag Berlin
319 Heidelberg 2013.
- 320 Ayorinde, T.T., Rabiou, A.B., and Amory-Mazaudier, C. (2016). Inter-hourly variability of Total
321 Electron Content during the quiet condition over Nigeria within the Equatorial Ionization
322 Anomaly region. *J. Atmos. Solar Terr. Phys.*, 145, 21 – 33.
- 323 Bagiya, M.S., Joshi, H.P., Iyer, K.N., Aggarwal, M., Ravin-dran, S., and Pathan, B.M. (2009).
324 TEC variations during low solar activity period (2005 – 2007) near the Equatorial Ionization
325 Anomaly Crest region in India. *Ann Geophys.*, 27, 1047 – 1057.
- 326 Bhuyan, P.K. and Borah, R.R. (2007). TEC derived from GPS network in India and comparison
327 with the IRI. *Advances in Space Res.*, 39, 830 – 840.
- 328 Bolaji, O. S., J. O. Adeniyi, S. M. Radicella, and P. H. Doherty (2012), Variability of total
329 electron content over an equatorial West African station during low solar activity. *Radio Sci.*, 47,
330 RS1001, doi:10.1029/2011RS004812.
- 331 Ciruolo, L., and Spalla, P. (2002). TEC analysis of IRI simulated data. *Adv. Space Res.*, 29, 6,
332 959 – 966.
- 333 Dabas, R.S., Singh, L., Lakshmi, D.R., Subramanyam, P., Chopra, P., Garg, S.C. (2003).
334 Evolution and dynamics of equatorial plasma bubbles: relationships to $\mathbf{E} \times \mathbf{B}$ drifts, post-sunset
335 total electron content enhancements, and equatorial electrojet strength. *Radio Sci.*, 38, doi:
336 10.1029/2001RS002586.



- 337 D'ujanga, F.M., Opio, P. Twinomugisha, F. (2017). Variation of total electron content with solar
338 activity during the ascending phase of solar cycle 24 observed at Makerere University, Kampala.
339 Space Weather: Longitude and Hemispheric Dependences and Lower Atmosphere Forcing,
340 Geophysical Monograph 220, First Edition. Edited by Timothy Fuller-Rowell,
341 EndawokeYizengaw, Patricia H. Doherty, and SunandaBasu. © 2017 American Geophysical
342 Union. Published 2017 by John Wiley & Sons, Inc.
- 343 Eyelade, V.A., Adewale, A.O., Akala, A.O., Bolaji, O.S. and Rabi, A.B. (2017). Studying the
344 variability in the diurnal and seasonal variations in GPS TEC over Nigeria. Ann. Geophys., 35,
345 701 – 710.
- 346 Fayose, R.S., Rabi, B., Oladosu, O., Groves, K. (2012). Variation of total electron content
347 (TEC) and their effect on GNSS over Akure. Nigeria, Applied Physics Research, vol 4, No. 2.
- 348 Hajra, R., Chakraborty, S.K., Tsurutani, B.T., DasGupta, A., Echer, E., Brum, C.G.M.,
349 Gonzalez, W.D., Sobral, H.A. (2016). An empirical model of ionospheric total electron content
350 (TEC) near the crest of the equatorial ionization anomaly (EIA). J. Space Weather Space Clim.,
351 6, A29, doi: 10.1051/swsc/2016023.
- 352 Kane, R.P. (2002). Some implications using the group sunspot number reconstruction. Solar
353 Phys., 205, 2, 383 – 401.
- 354 Kleusberg, A. (1986). Ionospheric Propagation Effects in Geodetic Relative GPS Positioning.
355 ManuscriptaGeodaetica. 11, 4, 256-261.
- 356 Okoh, D., Lee-Anne McKinnell, L., Cilliers, P., Okere, B., Okonkwo, C., Rabi, A.B. (2014).
357 IRI-vTEC versus GPS-vTEC for Nigerian SCINDA GPS stations. Advances in Space Research,
358 <http://dx.doi.org/10.1016/j.asr.2014.06.037>.



- 359 Ogwala, A., Somoye, E.O., Oyedokun, O., Adeniji-Adele, R.A., Onori, E.O., Ogungbe, A.S.,
360 Ogabi, C.O., Adejo, O., Oluyo, K.S., Sode, A.T. (2018). Analyses of Total Electron Content over
361 Northern and Southern Nigeria. *J. Res. and Review in Sci.*, 21 - 27
- 362 Onwumechilli, C.A., and Ogbuehi, P.O. (1964). *J. Atmos. Terr. Phys.*, 26, 894.
- 363 Rama Rao, P.V.S., Krishna, S.G., Prasad, J.V., Prasad, S.N.V.S., Prasad, D.S.V.V.D., Niranjan,
364 K. (2009). Geomagnetic storm effects on GPS based navigation. *Ann. Geophys.*, 27, 2101 –
365 2110.
- 366 Rama Rao, P.V.S., Krishna, S.G., Niranjan, K., Prasad, D.S.V.V.D. (2006a). Study of temporal
367 and spatial characteristics of L-band scintillation over the Indian low-latitude region and their
368 possible effects on GPS navigation. *Ann. Geophys.*, 24, 1567 – 1580.
- 369 Rama Rao, P.V.S., Krishna, S.G., Niranjan, K., Prasad, D.S.V.V.D. (2006b). Temporal and
370 spatial variations in TEC using simultaneous measurements from Indian GPS network of
371 receivers during low solar activity period of 2004 – 2005. *Ann. Geophys.*, 24, 3279 – 3292.
- 372 Suranya, P.L., Prasad, D.S.V.V.D., Niranjan, K., Rama Rao, P.S.V. (2015). Short term
373 variability in foF2 and TEC over low latitude stations in the Indian sector. *Indian J. of Radio and*
374 *Space Phys.*, 44, 14 – 27.
- 375 Somoye, E.O. (2010). Diurnal and seasonal variation of fading rates of E- and F-region echoes
376 during IGY and IQSY at the equatorial station of Ibadan. *Indian Journal of Radio and space*
377 *Physics*, 38, 194 – 202.
- 378 Somoye, E.O., Akala, A.O., Ogwala, A. (2011). Day-to-day variability of h'F and foF2 during
379 some solar cycle epochs. *Journal of Atmospheric and solar Terrestrial Physics*, 73, 1915 – 1922.



380 Tariku, Y.A. (2015). Pattern of GPS-TEC variability over low-latitude regions (African sector)
381 during the deep solar minimum (2008 to 2009) and solar maximum (2012 to 2013) phases. Earth,
382 Planets, and space. 67, 35.

383 Titheridge, J.E. (1974). Changes in atmospheric composition inferred from ionospheric
384 production rates. J. Atmos. Terr. Phys., 36, 1249 – 1257.

385 Wu, C.C., Liou, K., Shan, S.J., Tseng, C.L. (2008). Variation of ionospheric total electron
386 content in Taiwan region of the equatorial anomaly from 1994 – 2003. Adv. Space Res., 41, 611
387 – 616.

388 Zhang, S.R., Holt, J.M. (2008). Ionospheric climatology and variability from long-term and
389 multiple incoherent scatter radar observations: variability. Ann. Geophys., 26, 1525 – 1537.

390

391